

Optimal Daltonization by Spectral Shift for Dichromatic Vision

Hiroaki Kotera; Kotera Imaging Laboratory, Chiba, Japan

Abstract

This paper proposes a spectral-based image daltonization algorithm for the dichromats getting the best visibility against their color deficiencies. The proposed model extracts the visible and invisible spectra to dichromatic vision based on the projection theory of spectral space to/from 2-D dichromatic cone space.. First, the fundamental spectra C^* visible to the trichromats are captured from the conventional sRGB camera images by a pseudo-inverse projection..Second, the fundamental spectra C^*_{DIC} visible to the dichromats are obtained by operating the extended matrix R_{DIC} based on matrix-R theory. Thirdly, the lost spectra ΔC_{DIC} are calculated as the difference between C^* and C^*_{DIC} .

The key point in this paper is to make use of the lost spectra for image daltonization revived again. Though the lost spectra ΔC_{DIC} are invisible to dichromats if left alone, they are shifted into the visible spectral region and added to the the fundamental spectra C^* of source image. As a result, the dichromatic image visibility is dramatically improved.

The optimal spectral shift is determined to maximizing the spectral visibility for the dichromats and minimizing the visual gap from the normals. The proposed algorithm is designed to solve a contradictory demand to cope with both dichromats and normals.

The paper shows how the model works well for image daltonization better than the existing popular color blind simulators.

Introduction

Most of the color blind simulators have followed the Brettel-Vienot-Mollon's model [1], [2], [3], but take a troublesome procedure to find the corresponding color pairs between the 3D gamut for normals and the reduced 2D gamut for dichromats.

P.Capilla et al [4], simplified the corresponding pair procedure

with a systematic color transform model. Recently, Pardo and Sharma [5] further proposed an advanced 2-step model focusing on the opponent-color stage.

The popular color blind simulators are widely accepted, but any of them didn't deal with the spectral response analysis.

In the previous paper [6], the author proposed a spectral-based dichromatic vision model based on the "Matrix-R" theory extended to the 2-D dichromatic version. The new model clarified what regions in input spectra are visible or invisible to the dichromats and extracted the lost spectra as a difference in the fundamentals between the trichromats and the dichromats. The lost spectra interpreted the spectral background behind the color blindness and must be surely useful for the image daltonization. However, the first version model had a drawback of using expensive spectral image inputs.

This paper reports the improved 2nd version. It makes use of conventional sRGB image instead of spectral image and proposes an optimal daltonization algorithm toward maximizing the dichromatic visibility for their confusing colors and minimizing the visual gap from the normals at the same time.

Advanced Spectral-based Dichromatic Model

The new model simulates the colors viewed by dichromats and improves the visibilities for confusing colors according to the following core procedures.

- [1] Getting fundamentals from sRGB camera image
- [2] Extraction of visible and invisible spectra for dichromats
- [3] Optimal image daltonization by spectral shift

Fig.1 overviews the proposed model including the spectral-based daltonization process from conventional sRGB camera images. The key point lies in the optimal spectral shift for daltonization.

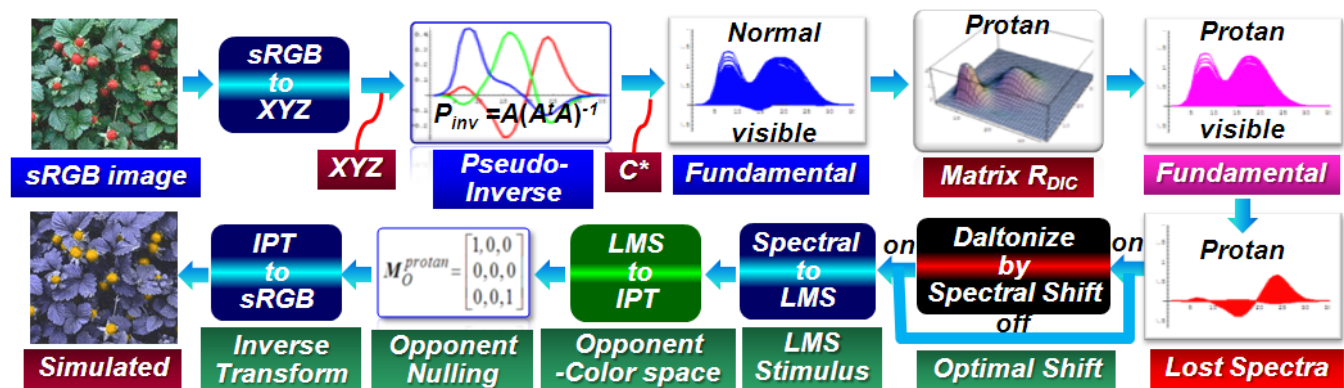


Figure 1 Overview of proposed model (in case of dichromatic vision for protanopes)

Getting Fundamental from sRGB Camera Image

Based on *Matrix-R* theory [7], the projection operator R_{LMS} to *LMS* cone space from n -dimensional spectral space, is given by

$$\begin{aligned} R_{LMS} &= A_{LMS} (A_{LMS}^t A_{LMS})^{-1} A_{LMS}^t \\ A_{LMS} &= [I(\lambda) \mathbf{m}(\lambda) \mathbf{s}(\lambda)]: \text{LMS cone sensitivity} \end{aligned} \quad (1)$$

In the *LMS* space, n -dimensional spectral input C is decomposed to the *fundamental* C_{LMS}^* and the *metameric black* B as

$$C = C_{LMS}^* + B, \quad C_{LMS}^* = R_{LMS} C, \quad B = (I - R_{LMS})C. \quad (2)$$

The fundamental C_{LMS}^* denotes the visible spectra to normal vision, while B is by-passed as the invisible spectra with zero tristimulus value.

Since the fundamental C_{LMS}^* carries the *LMS* tristimulus value T_{LMS} as same as the input spectra C , the following holds good.

$$T_{LMS} = A_{LMS}^t C = A_{LMS}^t C_{LMS}^*. \quad (3)$$

The 1st version model in the previous paper assumed to use a spectral input C in Eq. (2) to get the fundamental C_{LMS}^* . But it's impractical to use an expensive spectral camera for applying the model to the real scenes.

The 2nd version model uses the tristimulus value T_{LMS} instead of C . The fundamental C_{LMS}^* is exactly recovered from the tristimulus value T_{LMS} by the pseudo-inverse transform [8] of Eq. (3) as

$$\begin{aligned} C_{LMS}^* &= P_{LMS}^{inv} T_{LMS}, \\ \text{where, } P_{LMS}^{inv} &= A_{LMS} (A_{LMS}^t A_{LMS})^{-1}. \end{aligned} \quad (4)$$

Now, letting a calibrated sRGB tristimulus image be $sRGB_{img}$, its *LMS* tristimulus image is given by the linear transform as

$$LMS_{img} = (M_{XYZ \rightarrow LMS}) (M_{sRGB \rightarrow XYZ}) sRGB_{img}, \quad (5)$$

Substituting (5) for (4), the *LMS* fundamental image is obtained as

$$\begin{aligned} C_{LMSimg}^* &= P_{LMS}^{inv} LMS_{img} \\ &= P_{LMS}^{inv} (M_{XYZ \rightarrow LMS}) (M_{sRGB \rightarrow XYZ}) sRGB_{img}. \end{aligned} \quad (6)$$

Thus we can get the fundamental image for normals from sRGB camera images.

Extraction of Visible Spectra for Dichromats

Reducing the dimension of trichromatic matrix R_{LMS} in Eq. (1) from 3-D to 2-D, the matrix R_{DIC} extended to dichromatic version is given by

$$\begin{aligned} R_{DIC} &= A_{DIC} (A_{DIC}^t A_{DIC})^{-1} A_{DIC}^t \\ A_{DIC} &= A_{protan} = [\mathbf{m}(\lambda), \mathbf{s}(\lambda)] \text{ for protan} \\ A_{DIC} &= A_{deutan} = [I(\lambda), \mathbf{s}(\lambda)] \text{ for deutan} \\ A_{DIC} &= A_{tritan} = [I(\lambda), \mathbf{m}(\lambda)] \text{ for tritan} \end{aligned} \quad (7)$$

Fig.2 illustrates the extended dichromatic matrix R_{DIC} .

The dichromatic fundamental C_{DIC}^* is obtained by operating the projector R_{DIC} on the trichromatic fundamental C_{LMS}^* as

$$\begin{aligned} C_{DIC}^* &= R_{DIC} C = R_{DIC} C_{LMS}^* \\ &= C_{protan}^* \text{ or } = C_{deutan}^* \text{ or } = C_{tritan}^* \\ C_{protan}^* &= [A_{protan} (A_{protan}^t A_{protan})^{-1} A_{protan}^t] C_{LMS}^* \\ C_{deutan}^* &= [A_{deutan} (A_{deutan}^t A_{deutan})^{-1} A_{deutan}^t] C_{LMS}^* \\ C_{tritan}^* &= [A_{tritan} (A_{tritan}^t A_{tritan})^{-1} A_{tritan}^t] C_{LMS}^* \end{aligned} \quad (8)$$

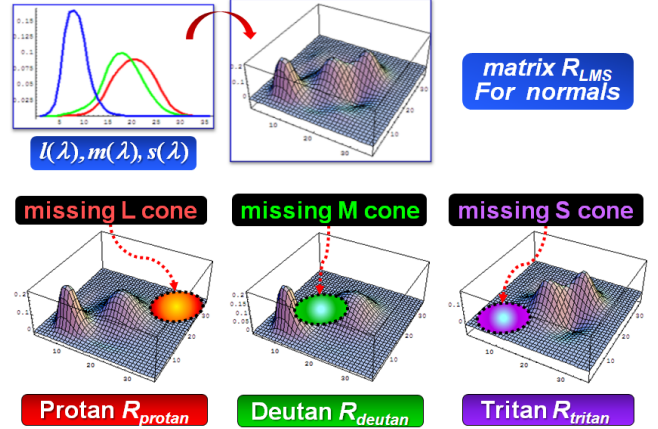


Figure 2 Extended projection matrix R_{DIC} for dichromats

The fundamental C_{DIC}^* denotes the spectra visible to dichromats. Thus, the difference in the fundamentals between normals and dichromats gives the lost spectra for dichromats against normals as

$$\Delta C_{DIC} = C_{LMS}^* - C_{DIC}^* = (R_{LMS} - R_{DIC}) C_{LMS}^*. \quad (9)$$

Fig.3 shows the visible and invisible lost spectra to dichromats (protan) for Macbeth color checkers in comparison with normal vision. It is notable that the lost spectra include the negative responses just corresponding to the *opponent-color* components of *red-green* for protan or *deutan* and *yellow-blue* for tritan.

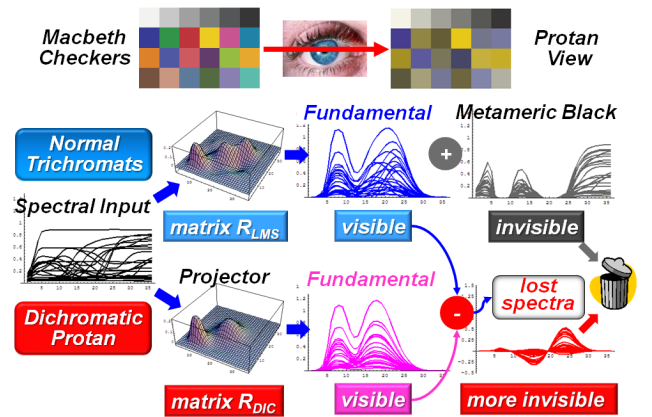


Figure 3 Extracted fundamental spectra visible and invisible to dichromats

Both the trichromatic *matrix-R_{LMS}* and dichromatic *matrix-R_{DIC}* are the scale-invariant and illuminant-invariant identity mapping operators inherent to human vision. They have

the recursive mapping property as follows.

$$\mathbf{R}_{LMS} = \mathbf{R} = \mathbf{R}(\mathbf{R}) = \mathbf{R}(\mathbf{R}(\mathbf{R})) \cdots = \mathbf{R}^m = \mathbf{R}_{LMS}^m \quad (10)$$

$$\mathbf{R}_{DIC} = (\mathbf{R}_{DIC})^m, m = 2, 3, \dots, \infty \quad (11)$$

Now, substituting the *LMS* fundamental image \mathbf{C}_{LMSig}^* in Eq.(6) for the fundamental \mathbf{C}_{LMS}^* in Eq. (8), the fundamental spectral image \mathbf{C}_{DICimg}^* for dichromats is calculated from sRGB image as

$$\begin{aligned} \mathbf{C}_{DICimg}^* &= \mathbf{R}_{DIC} \mathbf{C}_{LMSig}^* \\ &= \mathbf{R}_{DIC} \mathbf{P}_{LMS}^{inv} (\mathbf{M}_{XYZ \rightarrow LMS}) (\mathbf{M}_{sRGB \rightarrow XYZ}) \mathbf{sRGB}_{img} \\ &= \left[\mathbf{A}_{DIC} (\mathbf{A}_{DIC}^t \mathbf{A}_{DIC})^{-1} \mathbf{A}_{DIC}^t \left[\mathbf{A}_{LMS} (\mathbf{A}_{LMS}^t \mathbf{A}_{LMS}) \right] \right] \cdot (\mathbf{M}_{XYZ \rightarrow LMS}) (\mathbf{M}_{sRGB \rightarrow XYZ}) \mathbf{sRGB}_{img} \end{aligned} \quad (12)$$

As a result, using a calibrated sRGB camera not spectral camera, the *fundamental* spectral image visible to dichromats is captured from outside scenes and applied to simulate the dichromatic color appearance on sRGB display.

As well, the lost spectral image components in dichromatic vision is calculated by Eq. (9) like as

$$\Delta \mathbf{C}_{DICimg} = \mathbf{C}_{LMSig}^* - \mathbf{C}_{DICimg}^* = (\mathbf{R}_{LMS} - \mathbf{R}_{DIC}) \mathbf{C}_{LMSig}^* \quad (13)$$

Simulation on Dichromatic Color Vision

According to the model in **Fig.1**, the colors seen by dichromats are simulated using sRGB images as follows.

[Step1] Getting Fundamental spectral Image from sRGB

The fundamental spectral image visible to dichromats is derived from sRGB image by Eq.(12).

[Step2] Getting Lost Spectra and Image Daltonization

The lost spectral image in dichromatic vision are calculated by Eq.(13) using the norml fundamental image and it's used for image daltonization as metioned later. The daltonization process maybe by-passed as the occasion demands.

[Step3] Opponent-Color Nulling Porcess

Following the cone response stage, the *LMS* stimulus is transferred to the next opponent-color stage encoded to a luminance-chrominance color signals. So many opponent-color models have been proposed, such as one-opponent-stage linear models by Ingling and Tsou, Guth's *ATD80*, Boynton, and two-opponent-stage linear models by De Valois, two-opponent -stage nonlinear models by Guth's *ATD95*, and so on. Here the opponent-color model IPT by Ebner & Fairchild [9] is introduced, because IPT is simple but excellent in its color-opponency, hue linearity and color uniformities.

Now, the fundamental spectral image \mathbf{C}_{DICimg}^* is transformed to the *LMS* tristimulus image

$$\mathbf{LMS}_{DICimg} = \mathbf{A}_{LMS}^t \mathbf{C}_{DICimg}^* \quad (14)$$

Here, after transforming to IPT color space and introducing the opponent-color nulling hypothesis by Capilla, the dichromatic opponent-color image is given by

$$\begin{aligned} \mathbf{IPT}_{DICimg} &= \mathbf{M}_O (\mathbf{M}_{LMS \rightarrow IPT}) \mathbf{S}_{IPT} \cdot \mathbf{LMS}_{DICimg} \\ \mathbf{M}_O &= \mathbf{M}_O^{protan/deutan}, \text{ or, } \mathbf{M}_O^{tritan} \\ \mathbf{M}_O^{protan/deutan} &= \begin{bmatrix} 1, 0, 0 \\ 0, 0, 0 \\ 0, 0, 1 \end{bmatrix}, \mathbf{M}_O^{tritan} = \begin{bmatrix} 1, 0, 0 \\ 0, 1, 0 \\ 0, 0, 0 \end{bmatrix} \end{aligned} \quad (15)$$

\mathbf{S}_{IPT} denotes the nonlinear scaling with power of 0.43 for each entry of $\mathbf{LMS}_{DICimg} \cdot \mathbf{M}_O$ works to nullify one of the opponent chromatic mechanisms either (red–green) for protanopes and deutenopes or (blue–yellow) for tritanopes.

[Step4] Inverse Transform to sRGB Display

Finally, the simulated colors for dichromatic vision are displayed on sRGB monitor by the inverse transforms as

$$\mathbf{D}_{sRGBimg} = (\mathbf{M}_{sRGB \rightarrow XYZ})^{-1} (\mathbf{M}_{XYZ \rightarrow LMS})^{-1} \cdot (\mathbf{M}_{LMS \rightarrow IPT})^{-1} \mathbf{IPT}_{DICimg} \quad (16)$$

Optimal Daltonization using Lost Spectra

Shift-Rotate-Left Algorithm

Though the lost spectra $\Delta \mathbf{C}_{DIC}$ is invisible if leaving as it is, it'll be used for daltonizing the dichromatic visibility by shifting its spectral distribution into the visible wavelength region according to the following processes **[P1]** and **[P2]**.

[P1] $\Delta \mathbf{C}_{DICimg}$ is converted to $\Delta \mathbf{C}_{SHTimg}$ after shifting by λ_{SH} in a manner of rotate-left as

$$\begin{aligned} \text{if } \lambda_{max} \geq \lambda \geq \lambda_{SHT} + \lambda_{min}, \\ \Delta \mathbf{C}_{SHTimg}(\lambda - \lambda_{SHT}) &= \Delta \mathbf{C}_{DICimg}(\lambda) \\ \text{else if } \lambda_{SHT} + \lambda_{min} > \lambda \geq \lambda_{min}, \\ \Delta \mathbf{C}_{SHTimg}(\lambda_{max} + \lambda_{min} + \lambda - \lambda_{SHT}) &= \Delta \mathbf{C}_{DICimg}(\lambda) \end{aligned} \quad (17)$$

[P2] A daltonized image is created by adding the shifted lost spectral image $\Delta \mathbf{C}_{SHTimg}$ to the fundamental of original *LMS* image in Eq.(6) like as

$$\mathbf{DAL} \mathbf{C}_{LMSig}(\lambda) = \mathbf{C}_{LMSig}^*(\lambda) + \Delta \mathbf{C}_{SHTimg}(\lambda) \quad (18)$$

Now, the shifted lost spectra $\Delta \mathbf{C}_{SHTimg}$ are put to practical use as the revived visible spectra again.

A Measure for Maximizing Dichromatic Visibility

Now the fundamental $\Delta \mathbf{C}_{SHTimg}^*$ for the shifted $\Delta \mathbf{C}_{SHTimg}$ means the visible spectra to dichromats (note the *superscript** denotes the fundamental, that is visible).

Hence a best shift wavelength $\lambda_{SHT} = \lambda_{FIT}$ is determined to maximize the evaluation function $\Psi_{FIT}(\lambda_{SHT})$ following the process **[P3]**.

[P3] The fundamental for each pixel g_j of $\Delta \mathbf{C}_{SHTimg}$ is given by

$$\Delta \mathbf{C}_{SHTimg}^*(\lambda, g_j) = \mathbf{R}_{DIC} \Delta \mathbf{C}_{SHTimg}(\lambda, g_j) \quad (19)$$

Although the fundamental $\Delta \mathbf{C}_{SHTimg}^*$ includes the negative and positive spectral responses corresponding to the shifted lost

opponent-color components, its power spectra is meaningful.

Now taking the squared norm of ΔC_{SHTimg} as

$$\|\Delta C_{SHTimg}^*\|^2 = \langle \Delta C_{SHTimg}^*(\lambda, g_j) \bullet \Delta C_{SHTimg}^*(\lambda, g_j) \rangle, \quad (20)$$

Where, $\langle \bullet \rangle$ denotes the inner product.

$\Psi_{FIT}(\lambda_{SHT})$ is defined by the sum of Eq. (20) for all of the pixels $g_j(j=1\sim J)$ as

$$\Psi_{FIT}(\lambda_{SHT}) = \sum_{j=1}^J \|\Delta C_{SHTimg}^*(\lambda, g_j)\|^2. \quad (21)$$

A Measure for Minimizing Visual Gap between Normals and Dichromats

In addition to the visibility maximization, another demand may arise for minimizing the visibility difference between the normals and dichromats. This requirement is solved by defining the second evaluation function $\Psi_{DIF}(\lambda_{SHT})$ according to the process [P4].

[P4] The visible spectral difference between the normals and the dichromats after daltonization is calculated by operating the matrix- R_{LMS} and the matrix- R_{DIC} on Eq. (18) and applying Eq. (13) as follows.

$$\begin{aligned} \Delta C_{DIFimg}(\lambda) &= (R_{LMS} - R_{DIC})_{DAL} C_{LMSimg}(\lambda) \\ &= (R_{LMS} - R_{DIC})(C_{LMSimg}^*(\lambda) + \Delta C_{SHTimg}(\lambda)). \quad (22) \\ &= \Delta C_{DICimg}(\lambda) + (R_{LMS} - R_{DIC})\Delta C_{SHTimg}(\lambda) \end{aligned}$$

As well, the second evaluation function $\Psi_{DIF}(\lambda_{SHT})$ is defined by summing up the squared norm of Eq. (22) for all of the pixels $g_j(j=1\sim J)$ as

$$\Psi_{DIF}(\lambda_{SHT}) = \sum_{j=1}^J \|\Delta C_{DIFimg}(\lambda, g_j)\|^2. \quad (23)$$

As the value of function $\Psi_{DIF}(\lambda_{SHT})$ goes down to zero, the visibility difference between the dichromats and normals decreases toward their color appearance matching.

Optimal Spectral Shift for Maximizing Visibility & Minimizing Difference from Normal Vision

The proposed algorithm is designed to cope with both demands for improving the visibility for dichromats and decreasing the difference from normals. A compatible solution to this contradictory requirement at a glance, is given according to the processes [P5] and [P6].

[P5] The total evaluation function $\Psi_{OPT}(\lambda_{SHT})$ is defined by combining both functions of $\Psi_{FIT}(\lambda_{SHT})$ and $\Psi_{DIF}(\lambda_{SHT})$ as

$$\begin{aligned} \Psi_{OPT}(\lambda_{SHT}) &= 0.5\{\Psi_{FIT}(\lambda_{SHT}) + 1 - \Psi_{DIF}(\lambda_{SHT})\} \\ &\text{for } 0 \leq \Psi_{FIT}(\lambda_{SHT}) \leq 1 \text{ and } 0 \leq \Psi_{DIF}(\lambda_{SHT}) \leq 1. \quad (24) \end{aligned}$$

Where, $\Psi_{DIF}(\lambda_{SHT})$ is reversed to take the maximum value at the minimum difference point.

[P6] The best shift wavelength λ_{OPT} is determined to maximize the function $\Psi_{OPT}(\lambda_{SHT})$ as

$$\lambda_{SHT} = \lambda_{OPT} \text{ for } \Psi_{OPT}(\lambda_{OPT}) = \max_{\lambda_{SHT}=0}^{\lambda_{BAND}} \{\Psi_{OPT}(\lambda_{SHT})\}. \quad (25)$$

Experimental Results

The simulations on dichromatic color vision with and without daltonization process are performed for the typical images in comparison with the most popular conventional blind simulator.

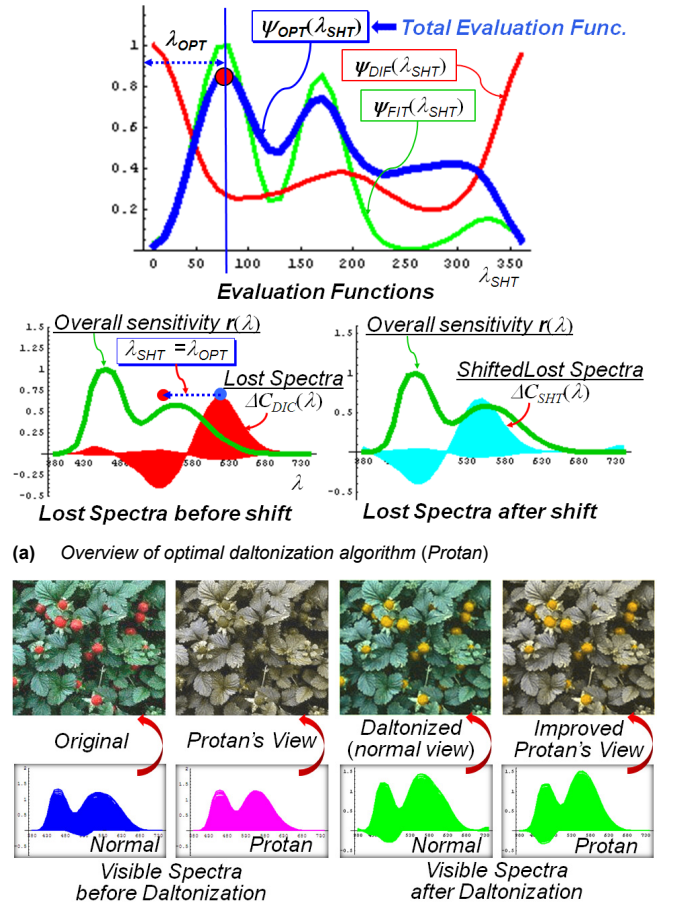
Fig.4 shows a result for protan with the “wild strawberry” image. (a) illustrates how the proposed optimal daltonization algorithm works to shift the lost spectra into the visible range matched to the overall dichromatic spectral sensitivity function.

The overall spectral sensitivity function $r(\lambda)$ for dichromats is simply defined as

$$\begin{aligned} r(\lambda) &= m(\lambda) + s(\lambda) \text{ for protan} \\ &= l(\lambda) + s(\lambda) \text{ for deutan} \\ &= l(\lambda) + m(\lambda) \text{ for tritan} \end{aligned} \quad (26)$$

The lost spectra automatically moves by the optimal shift wavelength $\lambda_{SHT} = \lambda_{OPT}$ given by Eq. (25) and matches $r(\lambda)$ as illustrated in the lower figures in (a).

The spectra exceeded the left end are relocated to the long-wavelength range in the right end in the manner of *shift-rotate-left*.



(b) Result corresponding to Fig. (a) applied to Protan

Figure 4 Optimal daltonization sample for Protan (“wild strawberry”)

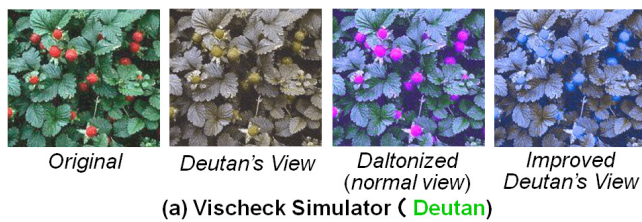
Very fortunately, as seen in the upper graphs in **Fig.4 (a)**, the function $\Psi_{FIT}(\lambda_{SHT})$ takes its maximum value at $\lambda_{SHT} = \lambda_{OPT}$ and simultaneously, the function $\Psi_{DIF}(\lambda_{SHT})$ is going down to a quasi-minimum point around at the same wavelength.

In this sample for **protan**, the **red** fruits of “wild strawberry” look to be almost the same **orange** color for both normals and protans, while the background **green** leaves look still different. Ideally, if the function $\Psi_{DIF}(\lambda_{SHT})$ takes the value ≈ 0 , the protan’s view will absolutely match with the normal’s. However the function $\Psi_{DIF}(\lambda_{SHT})$ tells us it’s impossible at present.

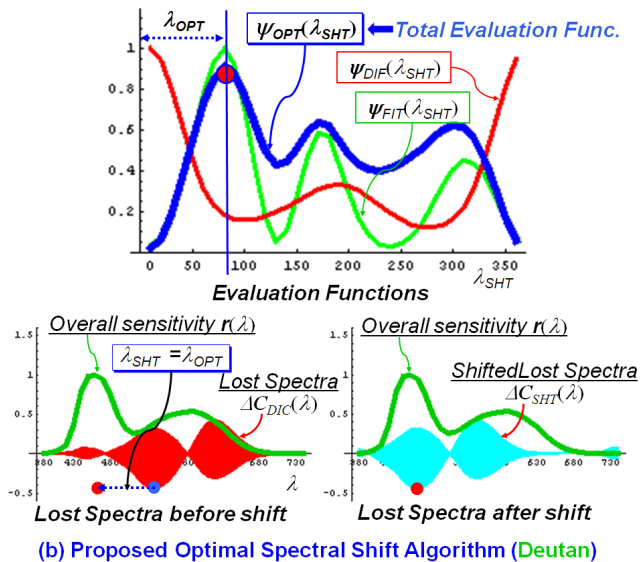
Fig.5 compares the daltonization effects for **deutan** using the same “wild strawberry” between the proposed model and the most popular conventional blind simulator Vischeck

The reddish fruits are hardly discriminable from the green leaves before daltonization, In the daltonized image in **Fig.5 (a)** by Vischeck, the reddish fruits are changed to bluish a little bit easy to discriminate, but still confusing with the background leaves, because the both areas are also changed into bluish.

While in the proposed model in **Fig.5 (b)**, the lost spectra is automatically shifted by $\lambda_{SHT} = \lambda_{OPT} \approx 80$ nm into the short wavelength region and added to the original fundamental spectra to create the daltonized image.



(a) Vischeck Simulator (Deutan)



(b) Proposed Optimal Spectral Shift Algorithm (Deutan)

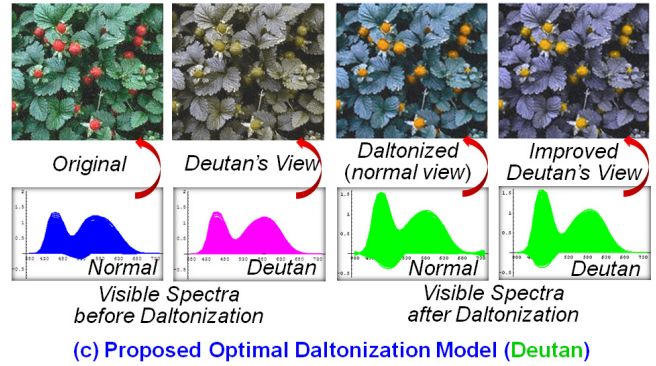


Figure 5 Comparison of daltonization effects in proposed vs Vischeck

In comparison with the case of **protan** in **Fig.4**, it’s worthy of notice that the visual spectral difference between normals and **deutans** is lesser decreased in **Fig.5**, because the function $\Psi_{DIF}(\lambda_{SHT})$ takes lower values in **Fig.5 (b)** than in **Fig.4 (a)**.

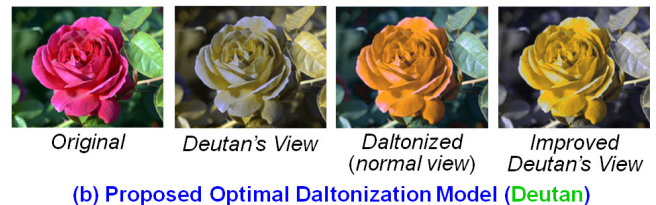
As clearly shown in **Fig.5 (c)**, the visual gap between the normal’s view and the deutan’s looks to be clearly reduced. Also in this case of **deutan**, the **red** fruits are clearly daltonized to visible **orange** dramatically distinguished from the background leaves much better than Vischeck in **Fig.5 (a)**.

Fig.6 is another result for **deutan** applied to a rose image “Dark Lady” including reddish and greenish confusing colors.

Vischeck simulator also worked nice in daltonization by changing the **reddish** petal into **magenta** for normals and **cyan** for deutans discriminable from the **grayish** leaves. While in the proposed model, the **reddish** petal is changed into **yellow-brown** both for normals and deutans and may be more natural than Vischeck.



(a) Vischeck Simulator (Deutan)



(b) Proposed Optimal Daltonization Model (Deutan)

Figure 6 Daltonization effects for “Dark Lady” in comparison with Vischeck

Fig.7 shows the furthermore daltonization results in **Ishihara** color blindness test plates for **deutan**. These plates include ambiguous color spectra very hard to discriminate for protan or deutan. **(a)** and **(b)** compare the the numeral figure “74” with confusing greenish colors. Vischeck worked to slightly improve the visibility as shown in **(a)** While the proposed model in **(b)** dramatically enhanced the visibility much better than Vischeck by shifting the lost spectra by $\lambda_{OPT} = 80$ nm.

Fig.7 (c) and **(d)** compare the more severe test. The numeral figure “29” marked with **reddish** dots pattern is hardly readable to

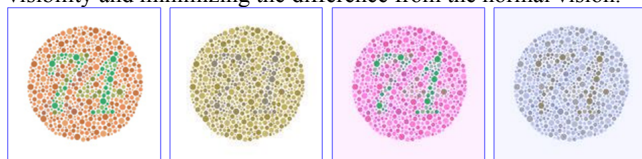
typical deutan even if after daltonization by Vischeck simulator as shown in (c). On the other hand, the proposed model improved it to be somehow readable as shown in (d).

Fig.8 is a practical sample applied to a “Tokyo Subway” root map. Though the reddish line colors are changed into magenta after daltonization by Vischeck, they must look to be “light blue” almost indistinguishable for deutan as shown in **Fig.8 (a)**.

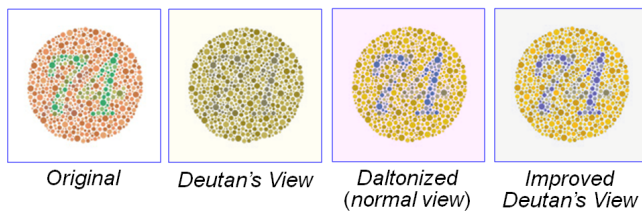
On the contrary, the proposed algorithm changes these reddish line colors into “brownish” distinguished from the other still staying “bluish” as shown in (b). The daltonization effect for protan by the proposed model is shown in (c). The confusing red-green opponent colors are also daltonized very well.

Through the all results in **Fig.5 ~ Fig.8**, the proposed model based on spectral-shift proved to work reasonable for improving the image visibility much better than the Brettel-based simulator.

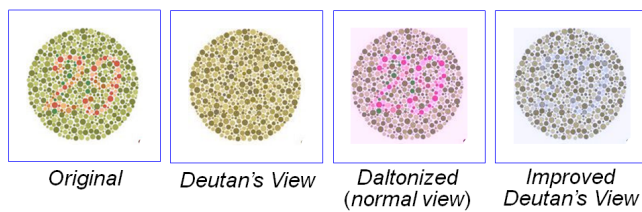
In particular, the proposed algorithm found a solution to meet the contradictory demands for maximizing the dichromatic visibility and minimizing the difference from the normal vision.



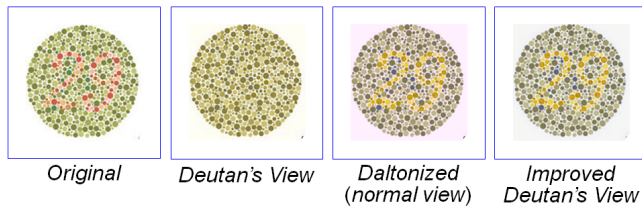
Original Deutan's View Daltonized (normal view) Improved Deutan's View
(a) Ishihara Plate “74” : Vischeck Simulator (Deutan)



(b) Proposed Optimal Daltonization Model (Deutan)



(c) Ishihara Plate “29” : Vischeck Simulator (Deutan)



(d) Proposed Optimal Daltonization Model (Deutan)

Figure 7 Daltonization for “Ishihara Plates” in comparison with Vischeck

Conclusions

The proposed color blindness simulation model is quite different from the conventional simulators. The conventional Brettel’s model searches the corresponding color pairs between 3D tri-color space and the reduced 2D dichromatic gamut plane.

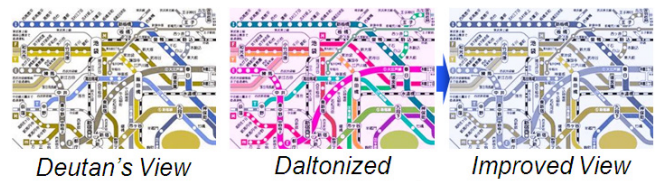
While, the novel model is based on the fundamental spectral responses derived from the extended dichromatic Matrix-R.

Since the 1st version in previous paper had a serious drawback using the expensive spectral images. The new version completely revised and advanced the model on the following points.

- [1] Capturing the fundamental spectra from sRGB images.
- [2] Image daltonization by spectral shift using the lost spectra
- [3] Optimal spectral shift algorithm for giving the best spectral matching to the surviving dichromatic sensitivity range.
- [4] Evaluation function to find the best spectral shift wavelength.

The proposed daltonization algorithm dramatically improved the dichromatic visibility in comparison with the representative color blindness simulator Vischeck.

Though the daltonized images are still unnatural for the normals, the proposed model worked well to minimize the visual difference between dichromats and normals. For example, the results in **Fig.8 (b)** and **(c)** suggest its possibility for the use of *subway root map or information map* and so on.



(a) Vischeck Simulator (Deutan)



(b) Proposed Optimal Daltonization Model (Deutan)



(c) Proposed Optimal Daltonization Model (Protan)

Figure 8 Application to “Tokyo Subway” map in comparison with Vischeck

The better daltonization algorithms are left behind as a future work toward more acceptable to both dichromats and normals.

References

- [1] F. Vie’not et al: What do colour-blind people see? , Nature 376 (1995) 127–128
- [2] H. Brettel et al: Computerized simulation of color appearance for dichromats, J. Opt. Soc. Am. A, 14, 10 (1997) 2641-265
- [3] F. Vie’not et al: Digital Video Color maps for Checking the Legibility of Displays by Dichromats, C. R. A., 24, 4 (1999) 243-252
- [4] P. Capilla et al: Corresponding-pair procedure: a new approach to simulation of dichromatic color perception, J. Opt. Soc. Am. A, 21,2, 176-186 (2004)
- [5] C. E. R. Pardo and G. Sharma: Dichromatic color perception in a two stage model: testing for cone replacement and cone

- loss models, Proc. IEEE IVMSP Workshop, 12-17 (2011)
- [6] H. Kotera: A Study on Spectral Response for Dichromatic Vision, Proc. CIC19, 8-13 (2011)
 - [7] J. B. Cohen, Visual Color and Color Mixture, Illinois Press (2001)
 - [8] H. Kotera et al: Recovery of Fundamental Spectrum from Color Signals, Proc. CIC4, 141-144 (1996)
 - [9] F. Ebner and M. D. Fairchild: "Development and Testing a Color Space (IPT) with Improved Hue Uniformity", Proc. CIC6, 8-13 (1998)

Author Biography

Hiroaki Kotera joined Panasonic Corp., in 1963. He received Doctorate from Univ. of Tokyo. After worked at Matsushita Res. Inst. Tokyo during 1973-1996, he was a professor at Dept. Information and Image Sciences, Chiba University until his retirement in 2006. He received 1993 IS&T journal award, 1995 SID Johann Gutenberg prize, 2005 IEEE Chester Sall award, 2006 ISJ journal award, 2007 IS&T Raymond. C. Bowman award, 2009 SPSTJ and 2012 IIEEJ best paper awards. He is a Fellow of IS&T.